INEEL/CON-02-00860
PREPRINT

Physical And Computational Modeling For Chemical And Biological Weapons Airflow Applications

Kelly J. Knight
Chris Barringer
Jon M. Berkoe
Glenn E. McCreery
Robert J. Pink
Donald M. McEligot

November 17, 2002

2002 ASME International Mechanical Engineering Congress And Exposition

Proceedings of IMECE'02:
2002 ASME International Mechanical Engineering Congress and Exposition
November 17-22, 2002, New Orleans, Louisiana

PHYSICAL AND COMPUTATIONAL MODELING FOR CHEMICAL AND BIOLOGICAL WEAPONS AIRFLOW APPLICATIONS

Kelly J Knight, Bechtel Corp. Research & Development, 1306 E. 17th St., Idaho Falls, ID 83404

Chris Barringer, Bechtel Corp. Research & Development, 7229 S. Alton Way, Englewood, CO 80112

Jon M. Berkoe, Bechtel Corporation Research & Development, 50 Beale St., San Francisco, CA 94105

Glenn E. McCreery, Idaho National Engineering and Environmental Laboratory, Idaho Falls, ID 83415-3885

Robert J. Pink, Idaho National Engineering and Environmental Laboratory, Idaho Falls, ID 83415-3885

Donald M. McEligot, Idaho National Engineering and Environmental Laboratory, Idaho Falls, ID 83415-3885

ABSTRACT

There is a need for information on dispersion and infiltration of chemical and biological agents in complex building environments. A recent collaborative study conducted at the Idaho National Engineering and Environmental Laboratory (INEEL) and Bechtel Corporation Research and Development had the objective of assessing computational fluid dynamics (CFD) models for simulation of flow around complicated buildings through a comparison of experimental and numerical results. The test facility used in the experiments was INEEL's unique large Matched-Index-of-Refraction (MIR) flow system. The CFD code used for modeling was Fluent, a widely available commercial flow simulation package. For the experiment, a building plan was selected to approximately represent an existing facility. It was found that predicted velocity profiles from above the building and in front of the building were in good agreement with the measurements.

INTRODUCTION

It is a huge challenge to protect a building or portion of a building against a terrorist attack involving the release of a chemical or biological weapon (CBW). There are many possible scenarios, including the release of internal or external agents. In the case of an external release, the agent will disperse into the atmosphere and potentially infiltrate a building or several buildings through air intakes and/or other leakage paths (e.g., doorways, windows, etc.). In the case of an internal release, the agent will disperse for some time in a room or hallway and then infiltrate the remainder of the building via the HVAC system or other leakage paths (open doors, deposition on people, etc.). Routes of entry for CBW agents, countermeasures for vulnerable areas, positioning of early warning detection and alarm systems, designation of safe areas within and outside a building, decontamination measures, etc., must all be addressed.

In such cases the mechanism by which the released agent is transported is airflow. The nature of the contaminated airflow, whether it be external winds or internal ventilated spaces, influences the transit times of the agent, its directions and destinations, and the degree of dilution and variability of concentration in the affected spaces. Thus, a predictive modeling tool that can realistically simulate airflow patterns inside and around buildings would provide valuable input to the design of any protection system. Accurate modeling of airflow patterns can lead to more effective mitigation measures.

Computational Fluid Dynamic (CFD) is such a tool, and in fact CFD simulations are becoming very common in engineering applications. The cost to perform experiments has steadily increased while computational expenses are decreasing. The increased computational capacity and availability allows engineers to quickly and evaluate existing problems and what-if scenarios. CFD codes can provide agent transport predictions in a timely manner for complex urban environments and buildings.

While the numerical algorithms are comprehensive, it is universally acknowledged that the modeling simplifications to keep CFD simulations tractable are not well suited for many complex flows. Also, proper grid resolution of almost all real world flows may not be obtainable for many years, requiring further simplifications. Boundary and initial conditions are a source of error in simulations and their effects on solutions must be examined closely. For example, the state of the art of CFD predicting flows over, around and through bluff bodies is still in an evolving stage [Rodi, *et al.*, 1997]. Though CFD has given us the opportunity to solve more complex problems, with the above shortcomings, it is always desirable to have the opportunity to compare CFD solutions to exact experimental data in order to evaluate and understand uncertainties in the flow and how they translate to the numerical model.

To assess the reliability of computer models for transport of chemical and biological agents, accurate measurements of the flow field must be made at carefully controlled, well known conditions for realistic geometries. Urban wind tunnel representations can provide useful results for a range of scales of urban terrain. To obtain flow measurements for coupled interior/exterior building flows in realistic surroundings, massive use of hotwire anemometry is required and/or optical techniques must be applied. There are well known difficulties in both measurement techniques that will not be delineated here since more comprehensive treatises on these difficulties are given elsewhere. An opportunity to apply a unique optical technique for such complex geometries exists with systems that match the refractive indices of the working fluid and the model. INEEL has recently placed in operation the world's largest MIR flow system. The MIR should be ideal for physical modeling and for assessment of computer models developed to predict external and internal building vulnerabilities to CBW attacks.

The present collaborative study has the objective of assessing the CFD code Fluent and its suite of turbulence models for simulation of flow around buildings through comparison of experimental and numerical results. Experiments have been conducted in the MIR test section and related numerical predictions were developed.

For the experiment, a scaled down building plan was selected to represent a typical building in an urban environment. Measurements with a two-component laser Doppler velocimeter (LDV) concentrated on the upstream flow conditions, flow above the building and separated flow in recirculating regions on the sides and aft of the building. Data included streamwise and vertical mean velocity components and their fluctuations, (U, V, u' and v') plus flow visualization by video and camera records of the paths of small bubbles.

An exact representation of the scaled down building and surroundings was created in a computational mesh for the CFD simulations. Evaluations of the turbulence models were completed with accompanying graphs of experimental versus computational data. A single simulation of an external agent release was completed. This latter simulation provides the context in which the results and conclusions of this research will be put with respect to building protection.

PHYSICAL MODELING

The goal of the current work was to test a widely used CFD code (Fluent) in its ability to predict the transport and fate of potential CBW agents around buildings. Consequently, accurate measurements of the flow field must be available for assessment at carefully controlled, well-known, realistic geometrical and environmental conditions.

Previous work has indicated:

- Boundary layers associated with airflow over buildings have impacts on the ability and, conversely, the inability to protect buildings from contaminant releases outside the buildings.
- The flow around building features significantly affects the maximum pressure differential between building interior and exterior. The maximum can be much larger than expected from momentum calculations.
- There are features associated with the flow that are independent of specific conditions yet give guidance to mitigation strategies.

The approach was straightforward. A quartz model of a typical building was constructed and used for measurements in the MIR facility. Both numerical and experimental methods were used to calculate and measure the velocity profiles at key locations. The separated boundary layer region above the building and other separated regions were investigated.

INEEL Matched-Index-of-Refraction Flow System

A unique opportunity to apply optical techniques for complex geometries exists with systems that match the refractive indices of the working fluid and the model. There is no distortion of light rays; they pass directly through the model and fluid without being bent (Snell's Law). An advantage of such systems is that flow patterns, particle transport and velocities can be measured *inside and around* complex arrangements of transparent building models without disturbing the flow and without experimental uncertainties caused by distortion. INEEL's MIR facility has advantages that include:

- Does not disturb the flow
- Avoids optical distortion and related problems
- Measures normal component and its products ($\overline{uv}$) close to the surface (e.g., $y^+ \approx 0.1$)
- Good spatial and temporal resolution
- Good signal-to-noise ratio near surfaces

The innovative advantage of the INEEL system is its large size, leading to improved spatial and temporal resolution compared to others. To date most other systems with index matching capability have been small, with characteristic lengths of five cm or less. In contrast, the INEEL MIR flow test section has a cross section of about 60 cm x 60 cm and is about two meters long. This size allows the use of models of substantial size; the model in this project being one example. Since the system volume is over 11,400 liters, a light mineral oil was selected as the working fluid due to environmental and safety considerations. The oil's refractive index matches that of some quartz. The design flow rate can give unit Reynolds numbers up to about 1.7 x 10^5 per meter. The refractive index of the fluid is maintained at the desired value by a parallel temperature control system that maintains a constant temperature within the test section to within 0.1 C.

Currently, velocity and turbulence measurements are obtained with a two-component, TSI fiber optic based laser Doppler velocimeter mounted on a three-directional traverse controlled by the TSI software or manually [Durst, Melling and Whitelaw, 1981]. The diameter of its measuring volume is about 60 μm, giving spatial resolution (H/d) of about 1000 with a six cm model. The LDV is operated in the forward scattering mode to increase data sampling rates. Transmitting optics are provided by a Model 9832 two-component fiber optic probe for 514.5 and 488 nm, with lenses of various focal distances. Differential pressure transducers and manometers can measure flow speed and static pressure using several pitot-static probes and various wall static pressure taps. A recent experiment yielded data to a distance as near to the wall as $y^+ = 0.1$ and less [Becker, *et al.*, 2002]. Thus, it was possible to estimate the local apparent wall shear stress accurately from the **measured** gradient $\partial U/\partial y$.

Experimental Apparatus and Procedures

The experiment was designed to represent an appropriate building in a semi-urban environment. The model was mounted on a plate simulating flat terrain and the sidewalls of the test section induce blockage and boundary layers as from nearby buildings. Upstream, a turbulence generating "fence" was installed to provide the effects of the wakes of upstream buildings. The consequent velocity profile approaching the building corresponded to a redeveloping profile below a low atmospheric jet [Scorer, 1958] displaced upwards by the building complex.

The scaled building model was machined from a solid block of quartz. Model thickness was approximately 60.5 mm. The model was mounted on an acrylic plastic sheet that encompassed the full width (60.96 cm) and length (2.44 m) of the test section. The fence was constructed of an approximately 33 mm by 33 mm square grid of square cross-section bars (6 mm by 6 mm). The height of the fence was approximately 100 mm.

The model building could be oriented at several angular displacements (yaw) with respect to the inlet flow. However, for the present experiments, the building's long axis was oriented parallel with the inlet flow. Two mounting positions for the model, Position 1, the more upstream position, and Position 2, the more downstream position, were used in the experiments. Position 1 allowed measurements to be collected along the downstream two-thirds of the model plus downstream of the model and far upstream of the model. Position 2 allowed measurements to be collected along the front half of the model plus upstream of the model.

The flow loop oil temperature was maintained at 23.7°C ± 0.1°C for all measurements. Pump speed was maintained at 400 RPM for measurements with the model in Position 1 (further upstream), and 425 RPM for measurements with the model in Position 2 (further downstream). Pump speed was maintained to within ±1 RPM.

Experimental Results

Measurements were collected at various locations adjacent to the model as well as upstream and downstream of the model. Each measurement data file consists of the statistical results of, typically, 10,000 individual measurements at each location. The data were collected and processed using the FIND version 1.4 software for the TSI LDV. The statistical results obtained from the FIND software were then transferred to Excel files for further analysis. The raw data files consisting of, typically, 10,000 U, V data pairs (where U = velocity in the X direction, and V = velocity in the Z direction) versus time were stored on the computer used for LDV processing. The Excel files contain measurement coordinates (X,Y,Z), number of data points, U and V velocities, u′ and v′ turbulence fluctuations, turbulence level, and other turbulence statistics.

The difference between the INEEL coordinate system and the Bechtel model coordinate system is given in Figure 1. The experimental measurements in this paper are given in the INEEL coordinate system.

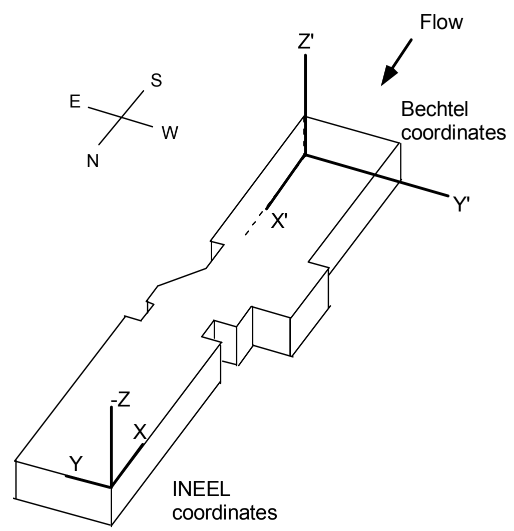

Figure 1. Coordinate systems and flow direction.

The Reynolds numbers (Re = U H/n) may be estimated for the two upstream flows based on free stream mean velocities, they would be about 6200 and 8300 for Positions 1 and 2, respectively. If based on the mean velocities at the height of the model, these values become Re ≈ 4840 and 5150. With either definition, the values are above the threshold for large scale similarity or Reynolds number independence [Snyder, 1981].

The spanwise uniformity of the inlet flow was investigated by obtaining vertical and horizontal traverses at various positions. As shown in Figure 2, measured values of the mean velocity U at any elevation Z for four spanwise locations lie within a range of ± two per cent, relative to the free stream magnitude. The horizontal distribution of the inlet flow is, therefore, quite uniform.

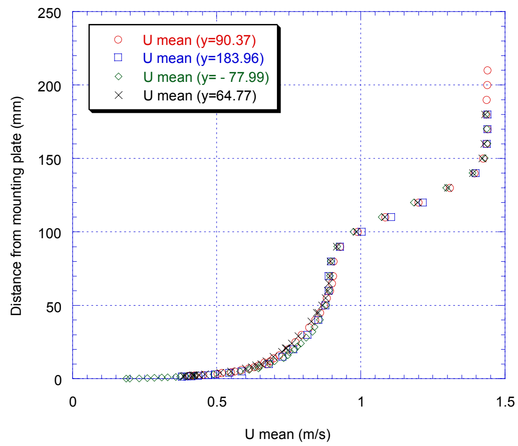

Figure 2. Vertical profiles of the mean streamwise velocity component upstream of the model.

The “roof” velocity profiles were obtained as vertical and axial traverses at mid-model positions in the horizontal direction. These profiles will be shown with the corresponding CFD profiles in the next section. Recirculation regions are evident in the profiles. The separation at the front edge [Scorer, 1968] is clearly shown in Figure 3.

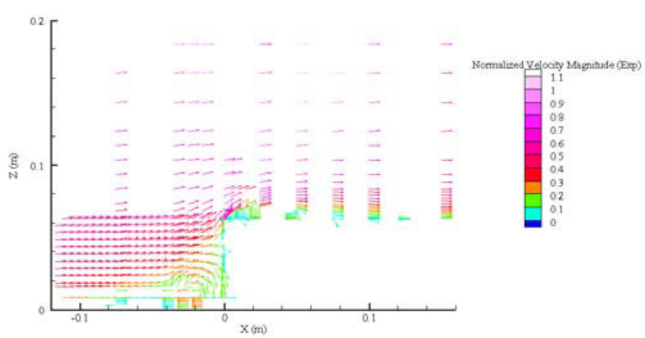

Figure3. A vector plot near the front edge of the model from experimental data.

Recirculation regions include eddies at the lower upstream face of the model, above the model downstream of the upstream face, a “separation bubble”, downstream of the upstream west and east corners of the upstream face, downstream of the downstream face and within the alcoves of the east and west walls. Approximately ten individual eddy regions are identified from the LDV data and from flow visualization videos and photographs. This number is only approximate because several eddy boundaries merge and are indistinct and transient. This observation is especially true of the small corner eddies, as distinct from the main corner eddies. The recirculation zones are shown schematically in Figure 4.

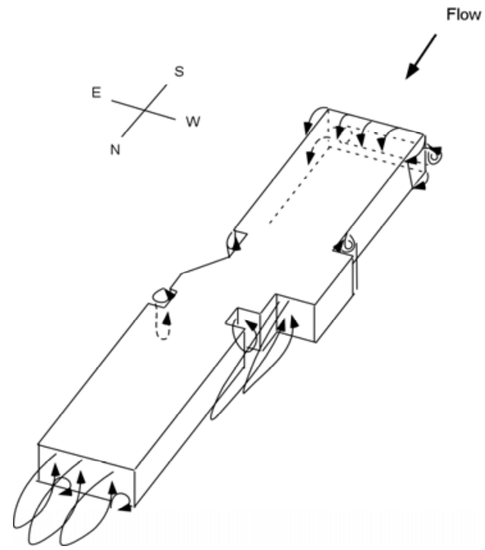

Figure 4. A schematic diagram of a few recirculation zones around the building.

More experimental results will be shown in the next section. It will be more instructive to discuss these results in the context of how the CFD predictions compare and the implications on building protection strategies.

COMPUTATIONAL MODELING

Objective

Many scientists and engineers do not have access to the robust CFD codes possessed and created by national labs and academia. Investigators must turn to commercially available codes. Fluent, a commercial CFD code, has been widely available for many years. It if of great interest to evaluate Fluent’s performance, in order to understand the context and accuracy of Fluent simulations and their bearing on actual conditions. This study was motivated by the need to evaluate Fluent’s capability to model the spatial and temporal evolution of potential CBW agents around, into and through buildings. Reliable predictions of the actual environmental flow around urban bluff bodies are needed for design of protective features.

The application of a CFD code to a given problem involves, among many others, two basic constraints: computational time and grid size. Only a few investigators have access to the large-scale teraflop machines that are available now. For the rest of us, solving engineering problems take place on mid to large size workstations, limiting the ability to resolve the flow properly both spatially and temporally. Work contracts to solve these problems can be as long as a year but more typically allow only few months or a few weeks to complete. With these time and computational constraints, it is not always possible to investigate the problem to the degree needed for a robust solution. Under these circumstances, CFD is a tool that provides insight into flows. The evaluation of the turbulence models done in this study provides some insight into the behavior of the flow and the effects of model assumptions on our understanding of flow characteristics.

CFD Code and Simulation Setup

Fluent is an unstructured solver based upon the Reynolds Averaged Navier-Stokes (RANS) equations, using a variant of the SIMPLE method for simulation solution. Fluent possesses the standard and SST k-ω model of Wilcox, 1993 and Mentor, 1994, respectively. The k-ε, Reynolds Stress and Spalart-Allmaras models are also available but not evaluated here. A comprehensive study done by Bardina, Huang and Coakley in 1997 showed results on the performance of four of the most common turbulence models (the Reynolds Stress model was not evaluated). Bardina, *et al.* and others have shown that the k-ε model was the worst in predicting separation. The SST model appeared to be the best overall model for solving complex flows. All models, however, do not do well on recovering flows downstream of reattachment and need better compressibility corrections for free shear flows. With these results in mind, this study uses the standard and SST k-ω models for turbulence.

Computational Mesh

Both versions of the k-ω model require the computational mesh to start in the interval of $1 \leq y^+ \leq 5$. The grid used for this study starts at $y^+ \approx 2$. These models also require that at least 10 nodes are placed in the boundary layer up to $y^+ = 100$. The size of our computers limited this resolution to about 3 nodes. (y^+ is the Reynolds number based upon the laminar friction velocity and the height above the surface)

Portions of the mesh were adapted using Fluent's mesh adaptation schemes in order to resolve the structures and areas of interest more fully. Not all areas were adapted properly or at all, again due to computational constraints.

Boundary Conditions

The velocity profile shown in Figure 2 was used at the inlet of the model. A uniform velocity was also used at the inlet to test the sensitivity on inlet conditions. It was found that the evolved profile produced much better results.

Simulation Results and Comparison to Experiment

Figure 5 shows the locations of where experimental data were taken. Comparisons to all of this data cannot be covered completely in this paper. The focus will be on the upstream portion of the flow near the building face and the farfield downstream traverses.

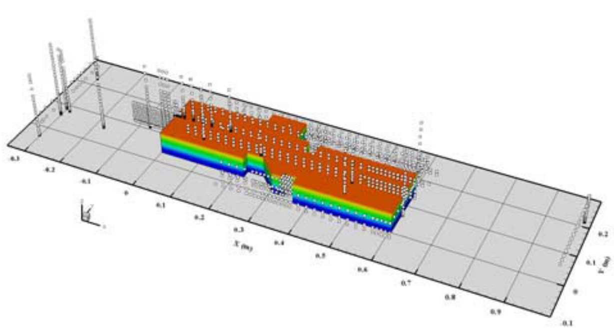

Figure 5. Locations of experimental data points.

The vector plot of the flow field, shown in Figure 3, is upstream of the building. It shows the behavior of the flow as the lower portion impacts the building, recirculates and progresses up and over the roof. There is separation of the flow at the edge of the roof due to the sharp change in curvature of the building boundary. Figure 6 shows contours of the velocity magnitude in the same plane at the same position as Figure 3.

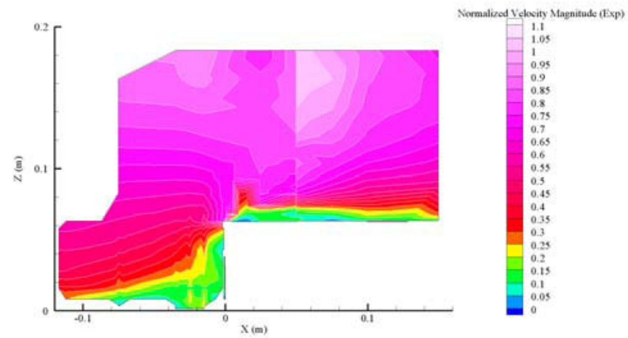

Figure 6. Contours of velocity magnitude at the front edge of the model from experiment.

Figures 7a and 7b show the same slice of data for the standard and SST k-ω models respectively. Though we will not spend time on the k-ε model, we show k-ε model data in Figure 7c for comparison.

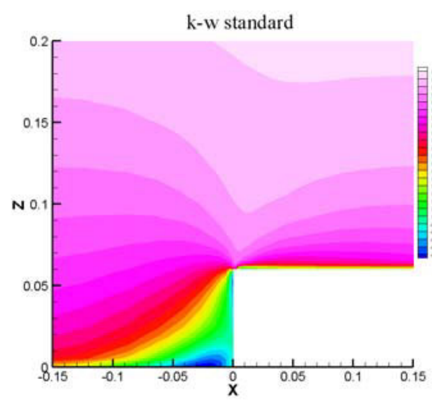

Figure 7a. Contours of velocity magnitude at the front edge of the model from the k-ω standard simulation.

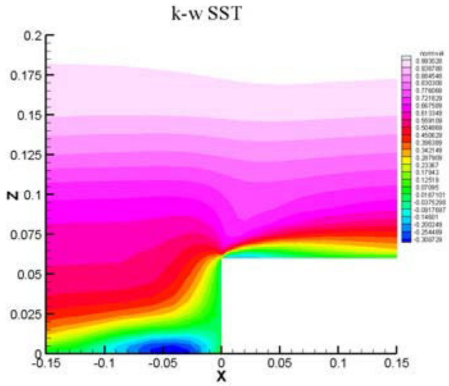

Figure7b. Contours of velocity magnitude at the front edge of the model from the k-ω SST simulation.

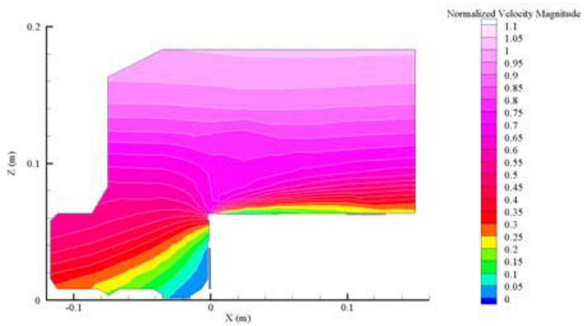

Figure 7c. Contours of velocity magnitude at the front edge of the model from the k-ε simulation.

The experiment shows curvature of the contours towards the building face at about mid height of the building. The two k-ω simulations show a similar shape while the k-ε does not capture the detail.

The velocity vectors from the two simulations are shown in Figures 8a and 8b. It can be seen that grid spacing is very coarse in the areas of recirculation and separation. This illustrates the improved detail that the k-ω SST model can provide versus other models on the same grid.

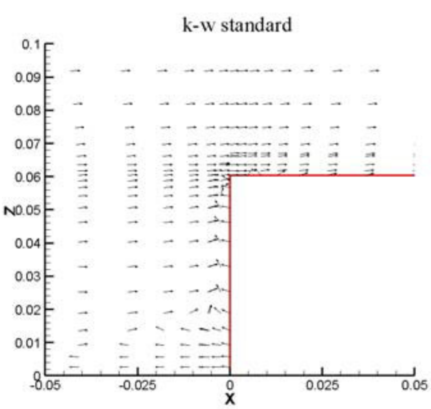

Figure 8a. Velocity vectors at the front edge of the model from the k-ω standard simulation.

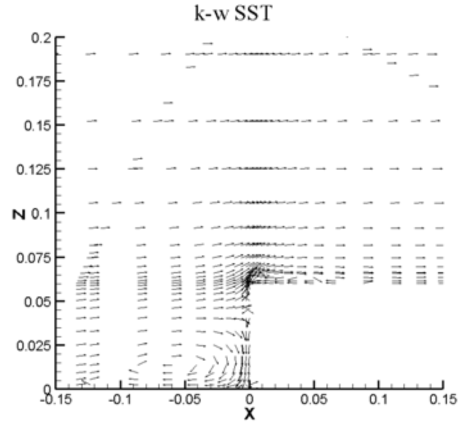

Figure 8b. Velocity vectors at the front edge of the model from the k-ω SST simulation.

The other key area for comparison is downstream of the building. The momentum is recovering from the separation caused by the building. There is not a comprehensive set of experimental data from which to make contours plots similar to what was done in Figure 6. The remaining figures will show profile comparisons.

Figure 9 shows the profiles of the axial velocity, U at 0.3 meters downstream of the rear face of the building. The SST model shows good agreement.

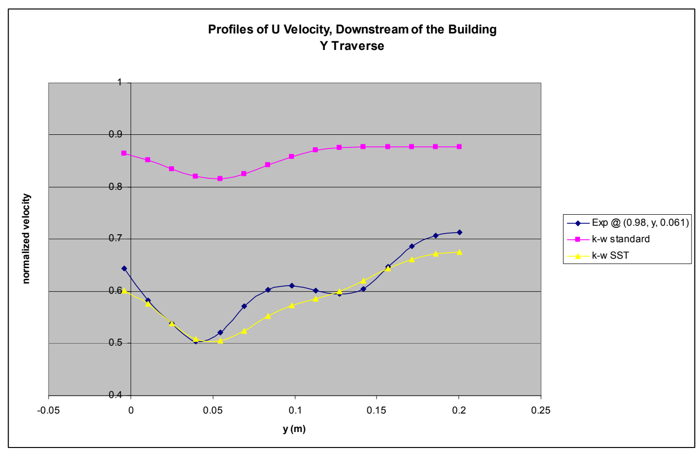

Figure 9. Velocity profiles of experiment and k-ω standard and k-ω SST models downstream of the building, a y coordinate traverse.

Figure 10 shows a vertical traverse of the axial velocity in the same downstream region as in Figure 9. Again the SST shows very good agreement.

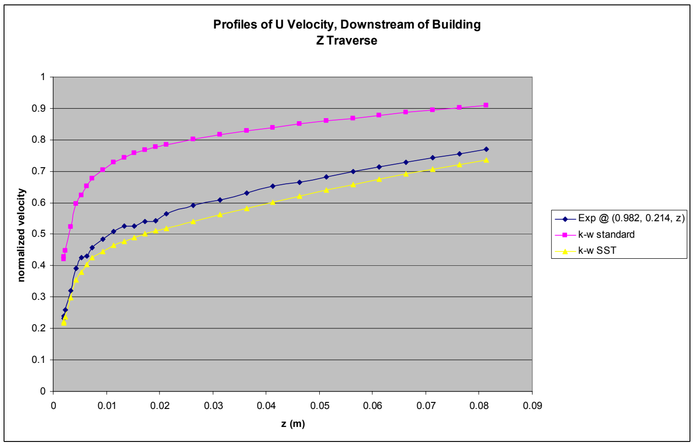

Figure 10. Velocity profiles of experiment and k-ω standard and k-ω SST models downstream of the building, a z coordinate traverse.

Accurate, predictive models can give information on flow variables of the flow that cannot be measured. The pressure field of the flow around the building can now be evaluated with a measure of confidence. Figures 11a, 11b, 12a and 12b show contours of pressure at two positions for the k-ω standard and SST models respectively. Figure 11a is the total pressure field at z = 0.03 m which is at mid-height of the building. Figure 11b shows the total pressure 10 mm above the building at z = 0.07 m. Figures 12a and 12b are at the same respective positions.

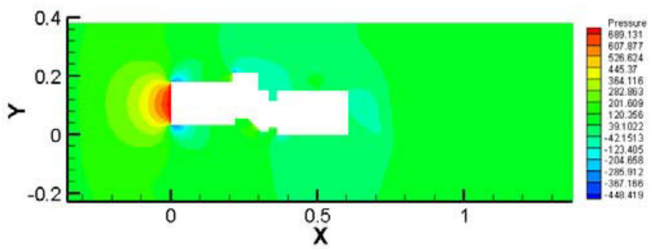

Figure 11a. Pressure contours at z = 0.03 m, mid-height of the building, k-ω standard model. Units are in pascals.

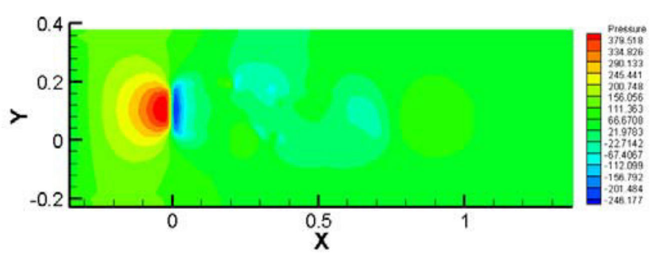

Figure 11b. Pressure contours at z = 0.07 m, just above the top of the building, k-ω standard model. Units are in pascals.

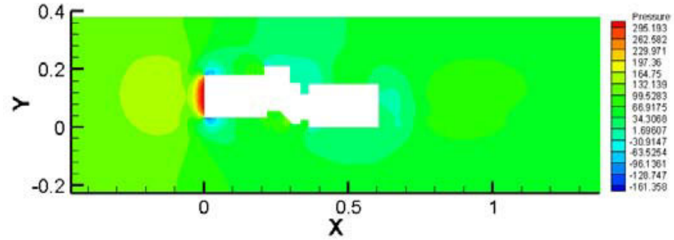

Figure 12a. Pressure contours at z = 0.03 m, mid-height of the building, k-ω SST model. Units are in pascals.

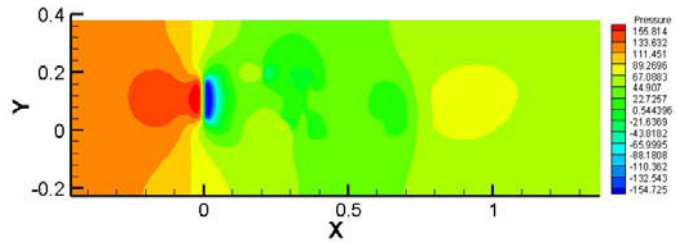

Figure 12a. Pressure contours at z = 0.07 m, mid-height of the building, k-ω SST model. Units are in pascals.

The differences shown in the pressure fields above helps solve a curious difference in the values that were calculated for U_∞ for each simulation. Several points of data were used to determine the average flow velocity in the free stream. The k-ω standard simulation had a lower velocity in the core of 1.3 m/s than the k-ω SST simulation that had 1.5 m/s as its average core velocity. The velocity vector plot in Figure 8a shows the flow essentially impacting the building directly. This creates a higher pressure front and therefore, more drag, reducing the momentum of the flow. This also affects the magnitude of the low pressure area just downstream of the roof edge where separation occurs. The k-ω standard shows higher values for the high pressure areas and lower values in the low pressure areas.

These results have direct bearing on the design of the outlet vents that are commonly placed on the roofs of buildings. These findings will also help evaluate the pressure differences felt by the interior of the building and subsequently the performance of the HVAC system for normal and emergency operation.

CONCLUDING REMARKS

CFD is a valuable modeling tool that has the potential for improving the accuracy of CBW threat assessments and improving the effectiveness of protection systems. The experiments demonstrated that use of the unique INEEL MIR flow system provides a means to assess capabilities of CFD codes proposed for the prediction of exterior flows and transport around realistic building shapes. The next logical step would be to use the MIR facility in conjunction with CFD to investigate coupled internal and external flow around a building. This could provide a comprehensive picture of the dependence of the interior flow field on exterior flow behavior.

ACKNOWLEDGMENTS

The experimental study at INEEL was funded by the Bechtel Corporate Funded Research and Development program under DoE Idaho Operations Office contract DE-AC07-99ID13727.

REFERENCES

Becker, S., C. M. Stoots, K. G. Condie, F. Durst and D. M. McEligot, 2002. LDA-measurements of transitional flows induced by a square rib. *J. Fluids Engineering*, in press.

Durst, F., A. Melling and J. H. Whitelaw, 1981. *Principles and practise of laser Doppler anemometry*. London: Academic Press.

Rodi, W., J. H. Ferziger, M. Breuer and M. Pouquie, 1997. Status of Large Eddy Simulation: Results of a workshop. *J. Fluids Engrg.*, 119, pp. 248-262.

Snyder, W. H., 1981. Guidelines for fluid modeling of atmospheric dispersion. Report EPA-600/8-81-009, Research Triangle Park, N. C.

Wilcox, D. C., 1993. Turbulence Modeling for CFD. DCW Industries, Inc., 5354 Palm Drive, La Cañada, Calif.

Menter, F. R. 1994. Two-Equation Eddy Viscosity Turbulence Models for Engineering Applications. *AIAA J.*, vol. 32, pp. 1299–1310.

Bardina, J. E., Huang, P. G., and Coakley, T. J., 1981. Turbulence Modeling Validation Testing and Development. NASA Technical Memorandum 110446, Ames research Center, CA.